A thermomechanical Hencky strain constitutive model for shape memory alloys

J. Wang[1], Z. Moumni[1], W. Zhang[2], W. Zaki[3]

[1] *IMSIA, Université Paris Saclay, {jun.wang,ziad.moumni}@ensta-paristech.fr*
[2] *ESAC, Northwestern Polytechnical University, ziad.moumni@nwpu.edu.cn*
[3] *Khalifa University of Science, Technology, and Research P.O. Box 127788, Abu Dhabi, UAE*

Abstract — This paper presents a new thermomechanically coupled constitutive model for polycrystalline shape memory alloys (SMAs) undergoing finite deformation. Three important characteristics of SMA behavior are considered in the development of the model, namely the effect of coexistence between austenite and two martensite variants, the variation of hysteresis size with temperature, and the smooth material response at initiation and completion of phase transformation. The formulation of the model is based on a multiplicative decomposition of the deformation kinematics into thermal, elastic and transformation parts. A Helmholtz free energy function consisting of elastic, thermal, interaction and constraint components is introduced. Constitutive and heat equations are derived from this energy in compliance with thermodynamic principles. The proposed model is then implemented in Abaqus/Explicit by means of a user-defined material subroutine (VUMAT). The results of numerical simulations are validated against experimental data obtained under a variety of thermomechanical loading conditions. The robustness and efficiency of the proposed framework are illustrated by simulating a SMA helical spring actuator.

Mots clés — constitutive model, thermomechanical coupling, Hencky strain, numerical simulation.

1 Introduction

Shape memory alloys (SMAs) are a class of smart materials capable of inelastic deformation that can be recovered under the influence of appropriate thermomechanical loadings. Over the last decades, substantial research was dedicated to developing constitutive models that can accurately describe the thermomechanical behavior of SMAs [Kan & Kang(2010), Lagoudas et al.(2012), Auricchio et al.(2014), Kelly et al.(2015)]. A large number of phenomenological models have been proposed in the literature with the various degrees of sophistication. Some of these models were shown to accurately describe complex SMA material responses such as asymmetry [Rizzoni & Marfia(2015)], multi-variant phase transformation [Auricchio et al.(2014)], strain localization [Bechle & Kyriakides(2016)], variation of transformation hysteresis [Lagoudas et al.(2012), Sedlák et al.(2012)], cyclic deformation [Yu et al.(2015a), Kimiecik et al.(2016), Kan et al.(2016)], crack growth [Baxevanis et al.(2015), Hazar et al.(2015)], rate dependence [Andani & Elahinia(2014), Yu et al.(2015b)], etc. However, most of these constitutive models disregard thermomechanical coupling [Xiao(2014)] and are limited to infinitesimal deformations [León Baldelli et al.(2015)].

In the present work, a thermomechanical constitutive model for large deformations of SMAs is developed, in which constitutive and heat equations are formulated in terms of Hencky strain. This strain measure, sometimes referred to as logarithmic or nature strain, is used in constitutive modeling of solids due to its remarkable properties in large deformations [Arghavani et al.(2011)]. Among the usual finite strain measures, the Hencky strain has two important features: (i) only Hencky strain maps the volumetric and isochoric parts of the deformation gradient onto the pure spherical and deviatoric strain measures, which allows straightforward additive split of the total strain [Xiao et al.(2004)] (ii) the logarithmic corotational rate of the Eulerian Hencky strain is the rate of deformation D [Reinhardt & Dubey(1996)], which makes it conjugate to the Cauchy stress in finite strain formulations. The model formulation is based on a multi-tier decomposition of deformation kinematics. In addition, the proposed model incorporates the following three important characteristics of SMA behavior that have not been concurrently

addressed in previous work: (i) effect of coexistence between austenite and two martensite variants; (ii) variation of the hysteresis size with temperature; (iii) smooth material response at the initiation and completion of phase transformation.

2 Constitutive model

The model is developed based on the principle of virtual power (PVP) in compliance with the first (energy balance) and second (entropy inequality) laws of thermodynamics. The Helmholtz free energy function Ψ is written as

$$
\begin{aligned}
\Psi = {} & \frac{1}{2}K\delta^2 + \mu\|\bar{\boldsymbol{h}}_e\|^2 - 3\alpha K\delta(\theta - \theta_0) + e_0^A - \eta_0^A\theta + c_v\left[(\theta - \theta_0) - \theta\ln\left(\frac{\theta}{\theta_0}\right)\right] \\
& + \Delta\eta_t\left(\chi^M + \chi^S\right)(\theta - \theta_0) + g^t + \frac{1}{2}\mu_t\|\boldsymbol{h}_t\|^2 \\
& - \left[\zeta^M\chi^M + \zeta^S\chi^S + \zeta^{MS}\left(1 - \chi^M - \chi^S\right) + \zeta^t(h_0 - \|\boldsymbol{h}_t\|)\right],
\end{aligned}
\tag{1}
$$

where K and μ are volumetric and shear moduli, δ, $\bar{\boldsymbol{h}}_e$ and $\boldsymbol{h}_t$ are volumetric, elastic and transformation Eulerian Hencky strains; α and c_v are thermal expansion coefficient and specific heat capacity; e_0^A and η_0^A are reference internal energy and entropy at reference temperature θ_0; $\Delta\eta_t$ is the entropy difference; χ^M and χ^S are volume fractions of multi-variant and single-variant martensites; g^t denotes interaction energy of martensite and austenite and μ_t is transformation hardening modulus; ζ^M, ζ^S, ζ^{MS} and ζ^t are nonnegative Lagrangian multipliers; h_0 is transformation strain magnitude.

Substituting the Helmholtz free energy function (1) into the Clausius-Duhem form of entropy inequality gives the elastic constitutive equations as

$$
p = K\left[\delta - 3\alpha(\theta - \theta_0)\right] \quad \text{and} \quad \boldsymbol{s} = 2\mu\bar{\boldsymbol{h}}_e,
\tag{2}
$$

where p and $\boldsymbol{s}$ are hydrostatic and deviatoric stresses.

Then, the thermodynamic forces associated with multi-variant $\mathcal{A}_M$, single-variant $\mathcal{A}_S$ martensite transformations and martensite reorientation $\mathcal{A}_N$ are written as

$$
\mathcal{A}_M = -\Delta\eta_t(\theta - \theta_0) - f^t + \zeta^M - \zeta^{MS},
\tag{3}
$$

$$
\mathcal{A}_S = h_0\bar{\boldsymbol{M}}_e : \boldsymbol{N}_t - \mu_t h_0^2\chi^S - \Delta\eta_t(\theta - \theta_0) - f^t - h_0\zeta_t + \zeta^S - \zeta^{MS},
\tag{4}
$$

$$
\mathcal{A}_N = h_0\chi^S\left(\mathbb{I} - \boldsymbol{N}_t \otimes \boldsymbol{N}_t\right)\bar{\boldsymbol{M}}_e,
\tag{5}
$$

where $\bar{\boldsymbol{M}}_e$ is a Mandel stress, $\boldsymbol{N}_t$ denotes the direction of transformation strain; $\mathbb{I}$ is the fourth-order identity tensor and $\left(\mathbb{I} - \boldsymbol{N}_t \otimes \boldsymbol{N}_t\right)\bar{\boldsymbol{M}}_e$ represents the component normal to $\boldsymbol{N}_t$ of the mandel stress $\bar{\boldsymbol{M}}_e$; $f^t = \partial g^t/\partial\chi$ is a tangential transformation hardening function expressed in the following form:

$$
f^t = \kappa\tan^m\left[\frac{1}{2}(\xi_a\chi + \xi_b)\pi\right] + r,
\tag{6}
$$

where κ, m, ξ_a, ξ_b and r are material parameters.

The evolution equations for χ^M, χ^S and $\boldsymbol{N}_t$ are written as

$$
\dot{\chi}^M = \dot{\gamma}^M\frac{\mathcal{A}_M}{|\mathcal{A}_M|}, \quad \dot{\chi}^S = \dot{\gamma}^S\frac{\mathcal{A}_S}{|\mathcal{A}_S|} \quad \text{and} \quad \boldsymbol{D}_N = \dot{\gamma}\frac{\mathcal{A}_N}{\|\mathcal{A}_N\|}.
\tag{7}
$$

where $\dot{\gamma}^M$, $\dot{\gamma}^S$ and $\dot{\gamma}$ are nonnegative multipliers. The associated yield functions are given by

$$
\mathcal{F}_M = |\mathcal{A}_M| - Y_M, \quad \mathcal{F}_S = |\mathcal{A}_S| - Y_S \quad \text{and} \quad \mathcal{F}_r = \|\mathcal{A}_N\| - (\chi^S)^2 Y_r,
\tag{8}
$$

where Y_M, Y_S and Y_r are yield thresholds controlling, respectively, evolutions of χ^M, χ^S and $\boldsymbol{N}_t$.

Finally, the temperature evolution equation is written as

$$
c_v\dot{\theta} = h_v - \nabla\cdot\boldsymbol{q} + \omega\left(\dot{\gamma}\|\mathcal{A}_N\| + \dot{\gamma}^M|\mathcal{A}_M| + \dot{\gamma}^S|\mathcal{A}_S|\right) + \theta\Delta\eta_t\left(\dot{\gamma}^M\frac{\mathcal{A}_M}{|\mathcal{A}_M|} + \dot{\gamma}^S\frac{\mathcal{A}_S}{|\mathcal{A}_S|}\right),
\tag{9}
$$

where h_v and $\boldsymbol{q}$ are heat source and heat flux, ω denotes the ratio of intrinsic dissipation converted into heat.

3 Numerical simulation

The proposed model is implemented into the finite element analysis software Abaqus/Explicit by means of a user-defined material subroutine VUMAT. To demonstrate capabilities of the model, numerical simulations are carried out and compared to experimental data under a variety of thermomechanical loading conditions. Finite element simulation of a SMA helical spring actuator undergoing large deformations and temperature variation is also performed.

The first set of simulations is dedicated to pseudoelasticity under isothermal uniaxial tensile loading at temperatures of 298 K, 303 K and 313 K. Experimental data for a polycrystalline NiTi wire (50.8 at.% Ni, provided by Memry Corporation) reported by [Lagoudas et al.(2012)] is utilized for validation. In the simulations, the applied stress is increased from 0 to a maximum value of 700 MPa then removed, with the temperature maintained at a constant value.

Figure 1 shows comparisons between model predictions and the experimental data reported by [Lagoudas et al.(2012)]. The pseudoelastic stress-strain responses at constant temperatures of 298 K, 303 K and 313 K are, respectively, plotted in Figure1(a), (b) and (c). In addition, the evolution of the single-variant martensite volume fraction χ^S is presented in Figure 1(d). From the figures, it is seen that the proposed model captures the pseudoelastic behavior of the considered polycrystalline SMA with good accuracy. In particular, complete shape recovery is achieved upon unloading, a smooth response is observed at the initiation and completion of phase transformation, and the elastic modulus is found to depend on phase composition.
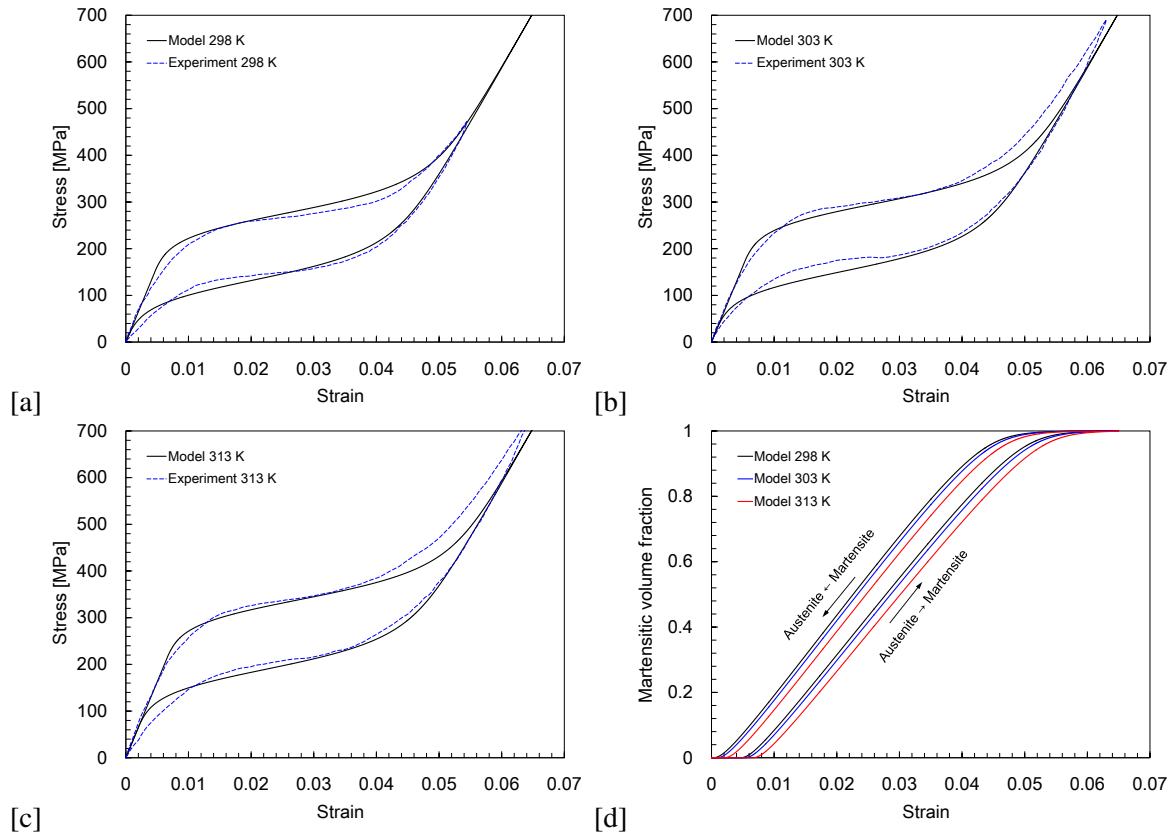

Figure 1: Model prediction vs. eperimental data under isothermal uniaxial tensile loading: (a) $\theta = 298$ K, (b) $\theta = 303$ K, (c) $\theta = 313$ K, (d) evolution of the single-variant martensite volume fraction.

Moreover, a biaxial strain-controlled butterfly-shaped loading test is investigated to demonstrate the reliability of the model in presence of multiaxial non-proportional loading conditions. Experimental data reported by [Grabe & Bruhns(2009)] is utilized as references. In the source work, $\gamma' = \gamma/\sqrt{3}$ and $\tau' = \sqrt{3}\tau$ are used as shear strain and stress measures for simplicity of a von Mises-type equivalence.

Figure 2 shows the butterfly-shaped strain input and the stress output in both axial and shear directions. The maximum axial and shear strain magnitudes reached in each case are $\varepsilon = \gamma/\sqrt{3} = 0.015$, as shown in Figure 2(a). The results of numerical simulation are compared to the reference experimental

data in Figure 2(b-d). Specifically, Figure 2(b) shows the scaled shear stress $\sqrt{3}\tau$ versus axial stress σ, Figure 2(c) shows axial stress σ versus axial strain ε and Figure 2(d) shows $\sqrt{3}\tau$ versus the scaled shear strain $\gamma/\sqrt{3}$. The overall agreement with the experimental data is satisfactory despite small deviation in presence of dominant shear and compression loadings. This is because the yield criteria for phase transformation and martensite reorientation of the von Mises type, which dose not account for the experimentally observed asymmetry in NiTi behavior in tension, compression and shear. A better simultaneous fit to tension, compression and shear data is achievable by means of more sophisticated criteria.
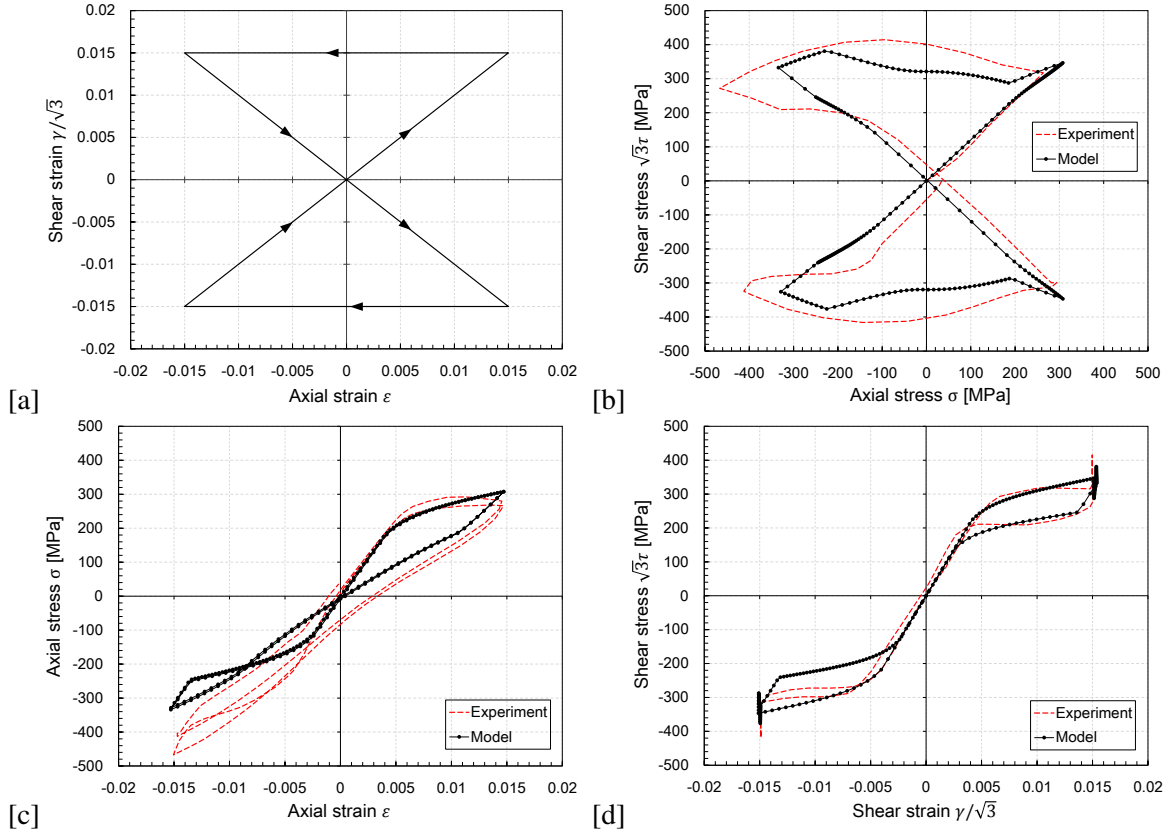

Figure 2: Comparisons between simulations using the present model and experimental data reported by [Grabe & Bruhns(2009)]: (a) butterfly-shaped axial-shear loading path, (b) shear stress vs. axial stress, (c) axial stress-strain response, (d) shear stress-strain response.

Finally, a SMA helical spring actuator is simulated to demonstrate the usefulness of the proposed model in analyzing complex structural SMA components subjected to non-trivial thermomechanical loading conditions. The SMA helical spring actuator adopted in the simulation has a coil diameter of 20 mm, a wire diameter of 2 mm and a spring pitch of 10 mm. Figure 3 shows the initial geometry, meshed using 3312 coupled temperature-displacement reduced integration hexahedral elements (Abaqus/Explicit C3D8RT). The element highlighted in red is chosen for studying the local material response, *i.e.* stress-strain behavior and phase transformation. The mesh of the cross-section adjacent to the red element is shown in the figure. Loading is applied at the nodes on end surfaces of the spring.

In the simulation, the spring is first preloaded with a force of magnitude 4 N in a smooth manner over a time period of 5 seconds at a constant temperature of 380 K. It is then cooled uniformly to 280 K before being uniformly heated back to 380 K over another time period of 5 seconds. Figure 4 shows contour plots of the von Mises stress and the martensite volume fraction χ in the spring at 280 K. The von Mises stress is maximum near the inner surface of the central portion of the spring as shown in Figure 4(a). In the same portion, the martensite volume fraction reaches its maximum value of magnitude 1 along toward the outside of the section, indicating complete transformation of austenite to martensite. The local stress response and phase transformation in the highlighted element (red in Figure 3) are shown in Figure 5(a). In the first half of the loading sequence, the von Mises stress increases with increased applied force to nearly 480 MPa. However, as the temperature is decreased from 380 K to 280 K at
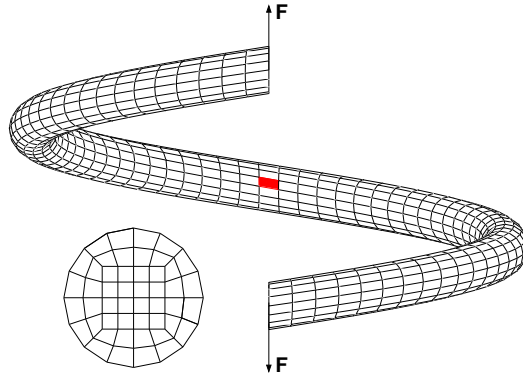
Figure 3: Geometry and mesh of the SMA helical spring actuator.

constant applied force, the von Mises stress decreases to 230 MPa and austenite completely transforms to martensite. When temperature is increased again to 380 K, the martensite finally transforms back to austenite. The displacement of the point of application of the load on the end surface is plotted versus temperature in Figure 5(b). At 380 K, the applied force of 4 N generates approximately 4 mm of elastic displacement. when temperature is decreased to 320 K, the formation of single-variant martensite results in significant transformation strain. The spring retrieves its original shape as the temperature is increased back to 380 K. The complete actuation cycle of the SMA helical spring actuator is shown in the figure.
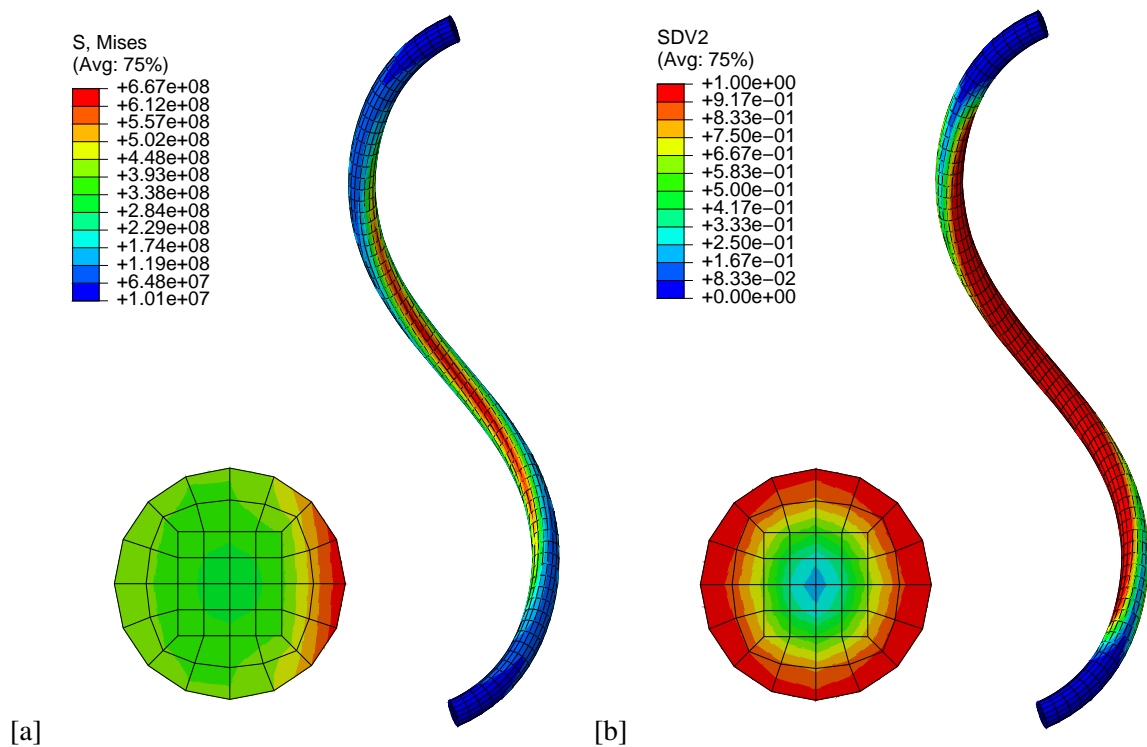

Figure 4: SMA helical spring actuator at temperature 280 K: (a) von Mises stress contour plot, (b) martensite volume fraction contour plot.

4 Conclusion

A thermomechanically coupled, Hencky-strain based constitutive model for shape memory alloys has been proposed in this work. A Helmholtz free energy function including elastic, thermal, interaction and constraint components has been introduced. Constitutive and heat equations were derived from the established Helmholtz free energy. Three important characteristics of SMA response are considered in
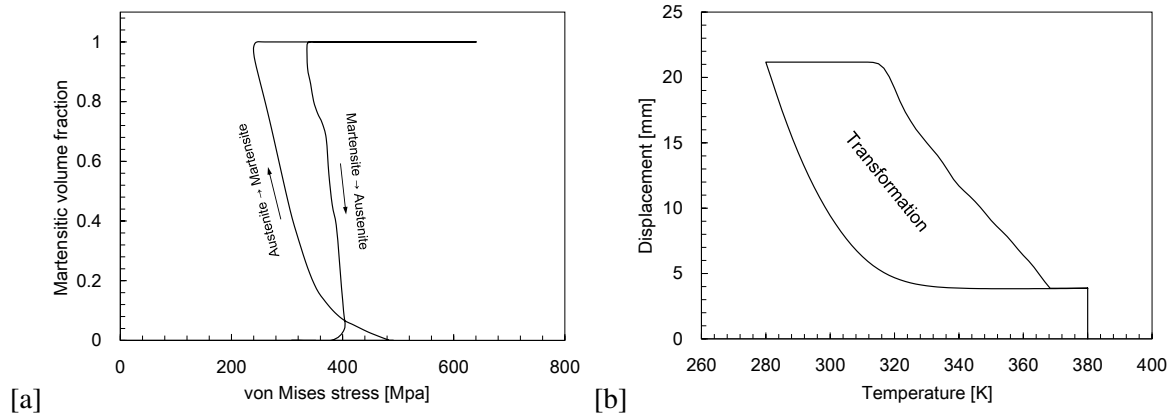
Figure 5: Temperature-induced actuation of the SMA helical spring actuator: (a) martensite volume fraction vs. von Mises stress curve for the selected element, (b) displacement vs. temperature curve at the point of application of the load on the end surface.

formulating the model. First, the effect of phase coexistence between austenite and two martensite variants is accounted for by deriving separate evolution laws of volume fractions for single-variant χ^S and multi-variant χ^M martensites, which can be active simultaneously. Then, the variation of the hysteresis size with temperature is characterized by means of the forward entropy difference $\Delta\eta_f$ and the reverse difference $\Delta\eta_r$. Finally, the smooth material behavior at initiation and completion of phase transformation is accounted for using a unique tangential transformation hardening function f^t. The model was then implemented into Abaqus/Explicit using a user-defined material subroutine VUMAT. Numerical simulations are carried out and validated against experimental data for a variety of loading cases, including proportional, non-proportional, isothermal, non-isothermal conditions. Finally, a simulation example is proposed in which a SMA helical spring is subjected to complex thermomechanical loading conditions.

References

[Andani & Elahinia(2014)] authorAndani, M. T., & authorElahinia, M. (year2014). titleA rate dependent tension–torsion constitutive model for superelastic nitinol under non-proportional loading; a departure from von Mises equivalency. *journalSmart Materials and Structures*, *volume23*, pages15012. 10.1088/0964-1726/23/1/015012.

[Arghavani et al.(2011)] authorArghavani, J., authorAuricchio, F., & authorNaghdabadi, R. (year2011). titleA finite strain kinematic hardening constitutive model based on Hencky strain: General framework, solution algorithm and application to shape memory alloys. *journalInternational Journal of Plasticity*, *volume27*, pages940–961. 10.1016/j.ijplas.2010.10.006.

[Auricchio et al.(2014)] authorAuricchio, F., authorBonetti, E., authorScalet, G., & authorUbertini, F. (year2014). titleTheoretical and numerical modeling of shape memory alloys accounting for multiple phase transformations and martensite reorientation. *journalInternational Journal of Plasticity*, *volume59*, pages30–54. 10.1016/j.ijplas.2014.03.008.

[Baxevanis et al.(2015)] authorBaxevanis, T., authorParrinello, A., & authorLagoudas, D. (year2015). titleOn the driving force for crack growth during thermal actuation of shape memory alloys. *journalJournal of the Mechanics and Physics of Solids*, *volume89*, pages255–271. 10.1016/j.jmps.2015.12.011.

[Bechle & Kyriakides(2016)] authorBechle, N. J., & authorKyriakides, S. (year2016). titleEvolution of localization in pseudoelastic NiTi tubes under biaxial stress states. *journalInternational Journal of Plasticity*, *volume82*, pages1–31. http://dx.doi.org/10.1016/j.ijplas.2016.01.017.

[Grabe & Bruhns(2009)] authorGrabe, C., & authorBruhns, O. T. (year2009). titlePath dependence and multiaxial behavior of a polycrystalline NiTi alloy within the pseudoelastic and pseudoplastic temperature regimes. *journalInternational Journal of Plasticity*, *volume25*, pages513–545. 10.1016/j.ijplas.2008.03.002.

[Hazar et al.(2015)] authorHazar, S., authorZaki, W., authorMoumni, Z., & authorAnlas, G. (year2015). titleModeling of steady-state crack growth in shape memory alloys using a stationary method. *journalInternational Journal of Plasticity*, *volume67*, pages26–38. http://dx.doi.org/10.1016/j.ijplas.2014.08.018.

[Kan & Kang(2010)] authorKan, Q., & authorKang, G. (year2010). titleConstitutive model for uniaxial transformation ratchetting of super-elastic NiTi shape memory alloy at room temperature. *journalInternational Journal of Plasticity*, *volume26*, pages441–465. 10.1016/j.ijplas.2009.08.005.

[Kan et al.(2016)] authorKan, Q., authorYu, C., authorKang, G., authorLi, J., & authorYan, W. (year2016). titleExperimental observations on rate-dependent cyclic deformation of super-elastic NiTi shape memory alloy. *journalMechanics of Materials*, *volume97*, pages48–58. 10.1016/j.mechmat.2016.02.011.

[Kelly et al.(2015)] authorKelly, A., authorStebner, A. P., & authorBhattacharya, K. (year2015). titleA micromechanics-inspired constitutive model for shape-memory alloys that accounts for initiation and saturation of phase transformation. *journalJournal of the Mechanics and Physics of Solids*, (pp. pages1–28). 10.1016/j.jmps.2016.02.007.

[Kimiecik et al.(2016)] authorKimiecik, M., authorJones, J. W., & authorDaly, S. (year2016). titleThe effect of microstructure on stress-induced martensitic transformation under cyclic loading in the SMA Nickel-Titanium. *journalJournal of the Mechanics and Physics of Solids*, *volume89*, pages16–30. 10.1016/j.jmps.2016.01.007.

[Lagoudas et al.(2012)] authorLagoudas, D., authorHartl, D., authorChemisky, Y., authorMachado, L., & authorPopov, P. (year2012). titleConstitutive model for the numerical analysis of phase transformation in polycrystalline shape memory alloys. *journalInternational Journal of Plasticity*, *volume32-33*, pages155–183. 10.1016/j.ijplas.2011.10.009.

[León Baldelli et al.(2015)] authorLeón Baldelli, A., authorMaurini, C., & authorPham, K. (year2015). titleA gradient approach for the macroscopic modeling of superelasticity in softening shape memory alloys. *journalInternational Journal of Solids and Structures*, *volume52*, pages45–55. 10.1016/j.ijsolstr.2014.09.009.

[Reinhardt & Dubey(1996)] authorReinhardt, W. D., & authorDubey, R. N. (year1996). titleApplication of objective rates in mechanical modeling of solids. *journalJournal of applied mechanics*, *volume63*, pages692–698.

[Rizzoni & Marfia(2015)] authorRizzoni, R., & authorMarfia, S. (year2015). titleA thermodynamical formulation for the constitutive modeling of a shape memory alloy with two martensite phases. *journalMeccanica*, *volume50*, pages1121–1145. 10.1007/s11012-014-0078-8.

[Sedlák et al.(2012)] authorSedlák, P., authorFrost, M., authorBenešová, B., authorBen Zineb, T., & authorŠittner, P. (year2012). titleThermomechanical model for NiTi-based shape memory alloys including R-phase and material anisotropy under multi-axial loadings. *journalInternational Journal of Plasticity*, *volume39*, pages132–151. 10.1016/j.ijplas.2012.06.008.

[Xiao et al.(2004)] authorXiao, H., authorBruhns, O., & authorMeyers, a. (year2004). titleExplicit dual stress-strain and strain-stress relations of incompressible isotropic hyperelastic solids via deviatoric Hencky strain and Cauchy stress. *journalActa Mechanica*, *volume168*, pages21–33. 10.1007/s00707-004-0074-5.

[Xiao(2014)] authorXiao, H. (year2014). titleAn explicit, straightforward approach to modeling SMA pseudoelastic hysteresis. *journalInternational Journal of Plasticity*, *volume53*, pages228–240. 10.1016/j.ijplas.2013.08.010.

[Yu et al.(2015a)] authorYu, C., authorKang, G., & authorKan, Q. (year2015a). titleA micromechanical constitutive model for anisotropic cyclic deformation of super-elastic NiTi shape memory alloy single crystals. *journalJournal of the Mechanics and Physics of Solids*, *volume82*, pages97–136.

[Yu et al.(2015b)] authorYu, C., authorKang, G., authorKan, Q., & authorZhu, Y. (year2015b). titleRate-dependent cyclic deformation of super-elastic NiTi shape memory alloy: Thermo-mechanical coupled and physical mechanism-based constitutive model. *journalInternational Journal of Plasticity*, *volume72*, pages60–90. 10.1016/j.ijplas.2015.05.011.